

# Natural-Graphite-Sheet Based Heat Sinks

Martin Cermak <sup>[1]</sup>, John Kenna <sup>[2]</sup>, Majid Bahrami <sup>[1]\*</sup>

<sup>[1]</sup> *Laboratory for Alternative Energy Conversion, School of Mechatronic Systems Engineering  
Simon Fraser University, 250-13450 102 Avenue, Surrey, British Columbia, V3T 0A3, Canada*

<sup>[2]</sup> *Terrella Energy Systems Ltd, Unit 11 - 32912 Mission Way, Mission, British Columbia, V2V 5X9, Canada*

\* Corresponding author – email: mbahrami@sfu.ca

## Abstract

Novel staggered plate fin heat sinks made of natural graphite sheets are presented and their performance is demonstrated via a direct comparison with aluminum. Measurements in a simple wind tunnel with a diode acting as a heat source show that the junction-to-ambient thermal resistance of the graphite heat sink is 31% lower when no electrically insulating thermal interface material (TIM) is used due to the lower thermal contact resistance (TCR). This offers a possibility to eliminate thermal grease in applications where electrical insulation is not required. With TIM both graphite and aluminum perform comparably. The graphite heat sink was less than half the weight of the aluminum one.

## Nomenclature

TIM – Thermal Interface Material  
TCR – Thermal Contact Resistance  
 $R_{INT}$  – Interface Thermal Resistance  
 $R_{SINK}$  – Heat Sink Thermal Resistance

## 1. Introduction

Graphite based materials are an attractive alternative to conventional thermal management materials such as aluminum or copper, due to their low density and high thermal conductivity. In the electronics cooling industry, thin sheets have become the most popular form of graphite. In comparison with metals, graphite sheets show high levels of anisotropy in their properties; e.g., thermal conductivity, electrical resistivity, and thermal expansion coefficient differ greatly between through-plane and in-plane. The magnitude of the properties is a function of many variables, but mainly of the manufacturing process. Thicker sheets with in-plane thermal conductivities ranging from 100 to 500 W/(m·K) [1][2] can be made from naturally occurring flake graphite in a process that involves mining, processing, exfoliation and compression. Thin sheets of high purity and structural quality, PGS (Pyrolytic graphite sheet), HOPG (Highly Oriented Pyrolytic Graphite), or TGS (Thermal Graphite Sheet), with thicknesses typically less than 100 $\mu$ m and in-plane thermal conductivities up to 1950 W/(m·K), are produced in significantly more complex processes that involve high temperature graphitization of carbon rich precursors [3].

Graphite sheets are most commonly used as heat spreaders in devices such as laptops [4], handheld devices [5], and plasma TVs [6], but other applications, including thermal interface material [7] and satellite radiator [8], can also be found in the literature. The idea of using graphite for heat sinks has been investigated by several researchers. In a study focused on natural convection heat sinks Icoz and Arik [9] compared several low-weight carbon based materials, including graphite

sheets, and, based on their figure of merit, reported that carbon foam was the most promising material and that the low through-plane thermal conductivity of graphite sheets does not limit the heat dissipation from the fin. The latter finding was confirmed by Sabatino and Yoder [10] in their numerical evaluation of pyrolytic graphite used as flat-plate thermal spreaders and finned heat sinks in circuit board applications.

The most relevant previous work can be found in a series of related publications that document a development of natural graphite based heat sinks for CPU cooling. The initial numerical simulation by Shives et al. [11] showed that low through-plane thermal conductivity limits the base plate spreading when the area of the heat source is smaller than the area of the base plate. In their other publication [12] they addressed this problem by introducing a hybrid heat sink which consisted of a copper base and graphite fins. Practical challenges encountered during the development of the heat sink were reported by Marotta et al. [13]. They faced mounting problems due to low strength of graphite and TCR problems due to uneven base plate surface. The former was solved by an aluminum frame while the latter was addressed by lapping the base plate surface.

In this work the viability of natural-graphite-sheet based heat sinks for power electronics cooling is explored. As typical for emerging technologies and materials, some of their properties are attractive while other require attention or even compromises. In the case of natural graphite sheets, the high thermal conductivity and low weight are certainly very attractive; many questions, however, arise when considering the anisotropy and mechanical properties. We believe that the anisotropy, at least in the case of the thermal conductivity, does

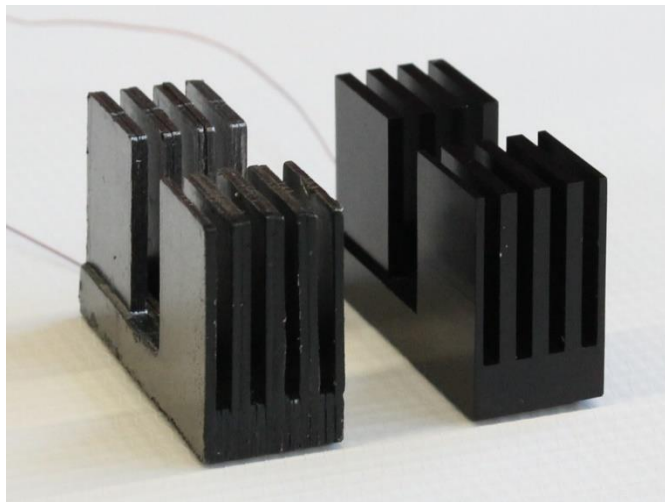


**Figure 1:** Graphite-sheet based (left) and anodized aluminum CNC machined (right) heat sinks

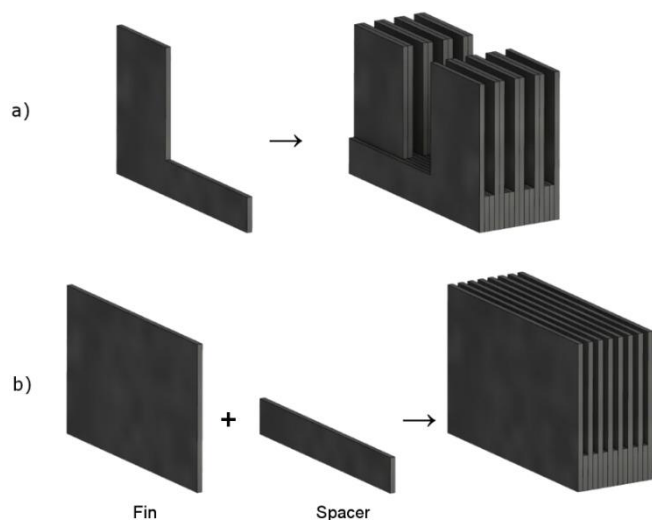


**Figure 2:** Heat sink assembly method a) Staggered layout  
b) Parallel plate layout

not pose any serious obstacle and only requires innovative thinking in the heat sink design instead of mimicking the conventional shapes typical for metals. The lower strength of the graphite sheets, which makes them fragile and brittle, can be a major problem in applications where sturdy and resilient heat sinks are necessary, but at the same time it is the very same property that allows easy manufacturing of virtually any shape and that also reduces the thermal contact resistance at the interface with other solids. The strength of graphite sheets can be improved by resin treatment, which, however, comes with higher hardness and thus higher TCR. TCR in metal-to-metal contacts is typically decreased by thermal greases or similar interface agents, which suffer from pump-out and dry-out problems. Replacing hard aluminum heat sinks with soft graphite ones in applications where electrical insulation is not required can offer a total elimination of the interface agents. Another interesting property of graphite that can be significant in harsh environments is its high corrosion resistance. In this study, we did not aim at demonstrating flexibility in manufacturing or testing of mechanical and other properties, instead we chose a simple geometry and focused on its thermal characterization. Due to the proof-of-concept nature of the study, a direct comparison of a graphite-sheet-based heat sink

and a geometrically identical aluminum one (Figure 1) was chosen as the most relevant first step for demonstrating the potential of our work.

## 2. Heat Sink Design

The graphite heat sink for this study was built by cutting a graphite sheet into L-shapes and stacking them in an alternating fashion (Figure 2a), thus forming a staggered plate fin configuration that was preferred to the parallel plate fin layout used by Marotta et al. [13] (Figure 2b), because it eliminates the spacers, which do not participate in heat dissipation and are therefore only a parasitic weight. Figure 2a also shows that only the side-most fins were made of a single sheet, while the rest consisted of two sheets and were therefore twice the thickness. This was done to increase the fin spacing, which reduces the pressure drop and lowers the risk of flow bypassing in non-shrouded conditions. The thickness of the graphite sheet was 1.2 mm and its thermal conductivity, which was estimated by measuring the density and using the correlations by Wei et al. [1], was 440 W/(m·K) in the in-plane direction and 5.9 W/(m·K) in the through-plane direction. The heat sinks were 50.8 mm long, 19.2 mm wide, and 31.8 mm high. The base plate was 7.6 mm thick and fins were 19.1 mm long.

## 3. Experimental setup

Heat sinks were tested in a simple wind tunnel that consisted of acrylic walls and an axial fan as shown in Figure 3. A power electronics diode (IXYS DSEI 30-06A), which served as a heat source, was mounted to the heat sinks by a bracket and two threaded rods. Plastic washers were added between the bracket and the nuts to reduce heat loss. This mounting method was chosen because the mechanical properties of graphite do not allow threaded holes in the base plate, which are necessary for the standard single-bolt method. The nuts were tightened to a torque of 0.1 N·m.

The fan and the diode were powered by two independent DC power supplies (Chroma 62012P-100-50 and 62012P-80-60) and the temperatures of the diode, heat sink and ambient air were measured by Omega 5SRTC T-type thermocouples read by a NI 9213 thermocouple module in a NI cDAQ-9178 data acquisition system at a 1 Hz sampling rate. To be able to measure the interface resistance the heat sink thermocouple was placed at the base near the diode as seen in Figure 4. A small hole for the thermocouple was drilled on the back side of

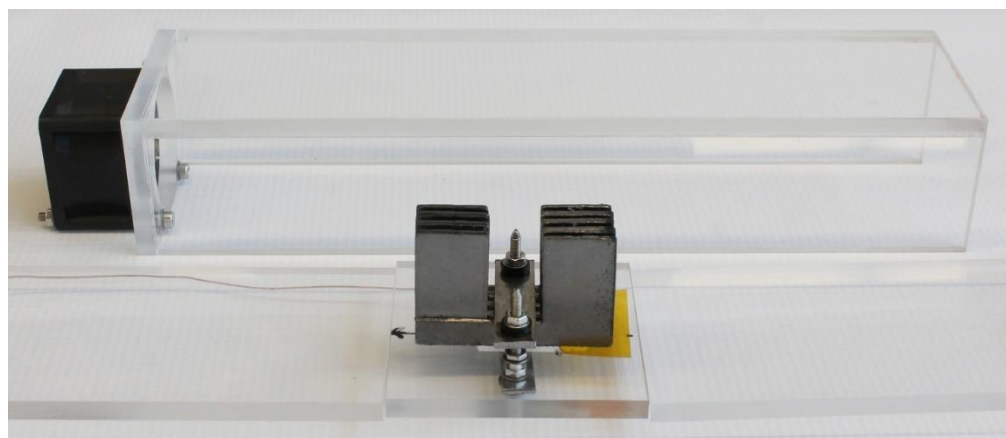


**Figure 3:** Wind tunnel - For clarity only the major parts are shown

the diode to ensure the correct junction temperature reading. Currents and voltages across the diode were measured to calculate the dissipated heat, which is required for the evaluation of thermal resistances. While the internal ammeter in the DC power supply can be used to measure the current, a separate voltage measurement at the diode terminals using a NI 9205 module was required to account for voltage drop in the cable.

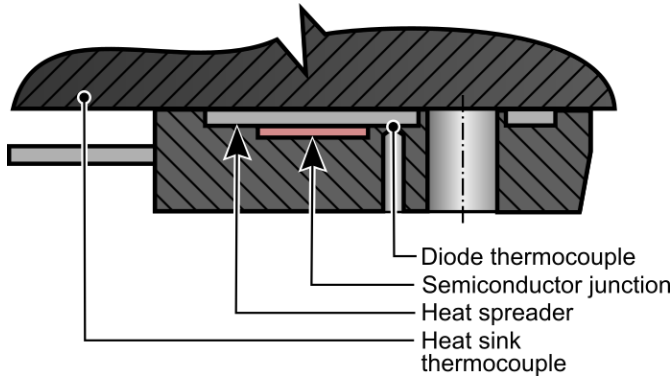


**Figure 4:** Section view of the diode and the heat sink with thermocouple locations

Both the DC power supplies and the data acquisition system were connected to a computer, which allowed the measurement to be fully automated with a LabVIEW interface. Based on a table with the desired test conditions (fan speed and diode power), the interface sets the current and voltage of the DC power supplies and evaluates the steady state by analyzing the reading from the diode thermocouple. The system was assumed to have reached the steady state when a slope of the line fit through the last 60 samples was smaller than  $0.001^{\circ}\text{C/s}$ . Once the steady state criterion was satisfied the interface wrote the averages and standard deviations of the measured values into a text file and then switched to the next test condition.

The air velocity at the center of the outlet was measured by Reed SD-4214 anemometer with default telescope probe.

#### 4. Measurements

The data for the thermal resistance calculations was collected for two levels of fan speed, three levels of diode power and for configurations with and without a 3M™ 8815 thermal interface material, whose role is to electrically insulate the diode and the heat sink. The location of the thermocouples allowed us to evaluate the contributions of the interface resistance  $R_{INT}$  and the heat sink resistance  $R_{SINK}$  to the total (junction-to-ambient) resistance  $R_{TOT}$  as

$$R_{INT} = \frac{T_{DIODE} - T_{SINK}}{\dot{Q}_{SINK}}, \quad R_{SINK} = \frac{T_{SINK} - T_{AMB}}{\dot{Q}_{SINK}},$$

$$R_{TOT} = \frac{T_{DIODE} - T_{AMB}}{\dot{Q}_{SINK}} = R_{INT} + R_{SINK}.$$

The heat dissipated by the heat sink  $\dot{Q}_{SINK}$  was calculated by

$$\dot{Q}_{SINK} = \dot{Q}_{DIODE} - \dot{Q}_{LOSS},$$

where  $\dot{Q}_{DIODE}$  is the diode power obtained by multiplying the measured voltage and current. To estimate the heat loss  $\dot{Q}_{LOSS}$  a separate measurement was performed in which a block of insulation material was clamped to the diode instead of the heat sink, which forced all the heat generated in the diode to leave through the bottom wall of the wind tunnel. Diode power and temperature were recorded and subsequently a line was fit through the data, which resulted in a simple relationship between the heat loss and the temperature of the diode:

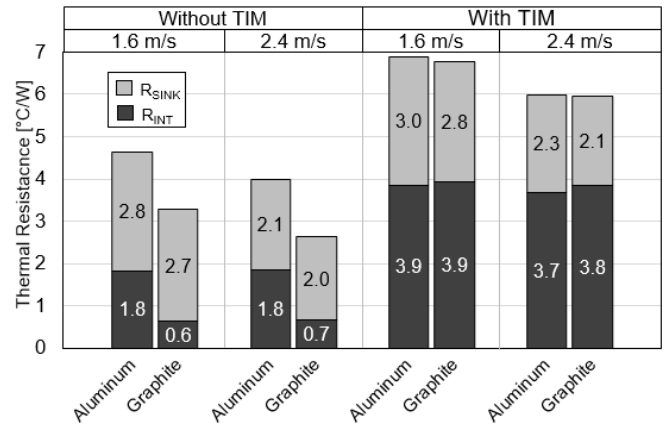


**Figure 5:** Summary of the thermal resistances; the total resistance corresponds to the total height of the bars while the light and dark grey parts correspond to the contributions of the heat sink and interface resistances, respectively. The anemometer readings in m/s are shown at the top.

$$\dot{Q}_{LOSS} = 0.04(T_{DIODE} - T_{AMB}) \quad [W].$$

#### 5. Results

The results, summarized in Figure 5, show that when no TIM is used the graphite heat sink performs better than the aluminum one, which can be explained by the lower hardness of graphite, as softer materials conform better to surface irregularities, which lowers their thermal contact resistance. When TIM is used between the heat sink and the diode, the effect of material hardness diminishes and the heat sinks perform comparably. The difference in the resistances in the case without TIM was significant, but in the case with TIM it falls within the uncertainty range. The uncertainty was estimated to be  $\pm 0.2^{\circ}\text{C/W}$  and  $\pm 0.1^{\circ}\text{C/W}$  for the interface and heat sink resistances, respectively. The repeatability of the data was investigated by twice dismounting and remounting the assembly with a new piece of TIM and the observed variations were incorporated in the uncertainty estimation.

The heat sink resistance, which is generally a function of the geometry and thermal conductivity, is comparable for all the measurements, with the maximum absolute difference  $0.2^{\circ}\text{C/W}$ . Since all the heat sinks in this study are geometrically identical the differences in the thermal conductivities of graphite and aluminum do not affect the thermal performance. Radiation heat transfer was considered negligible. The heat sink resistances are expected to differ more when the fin thickness is reduced, as the thermal-conductivity-dependent spreading and conduction resistances become more prominent, especially in the base plate, where the spreading is limited by the low through-plane thermal conductivity.

An indirect verification of the data can be made by comparing the interface resistance  $R_{INT}$  to the known value of the TIM resistance  $7.7^{\circ}\text{C}\cdot\text{cm}^2/\text{W}$  (from the manufacturer's specifications [14]). Multiplying the average interface resistance  $R_{INT}$  by the contact area yields  $9.5 \pm 2.2^{\circ}\text{C}\cdot\text{cm}^2/\text{W}$ , which is comparable to the reference value. The large uncertainty is due to the difficulty in estimating the contact area. Generally, the measured resistance was expected to be larger than the manufacturer's value because the interface

resistance includes also the resistances of the diode heat spreader and a part of the heat sink (Figure 4).

## 6. Conclusions

Geometrically identical heat sinks made of natural graphite sheet and aluminum were compared. In cases without TIM a 31% reduction in the total thermal resistance was seen, which led to 19% lower diode temperatures. When TIM was added between the diode and the heat sinks no significant difference in performance was observed. This behavior is explained by the difference in hardness of the heat sink material, which significantly affects the TCR. To reduce the TCR between components and metal heat sinks in applications where electrical insulation is not needed thermal grease or other forms of interface agents are used. Our results show that with graphite heat sinks it is possible to achieve the same without any pump-out or dry out. To make use of the potential of graphite-sheet-based heat sinks in applications where electrical insulation is required an alternative to conventional soft TIM's should be sought. One possibility is coating the heat sink with a thin insulating layer, which would offer an integrated solution and thus simplify the assembly process of the final device. The weight of the graphite heat sink was 20 g, which is only 44% of weight of the aluminum one (45.6 g). The lower weight is reflected in the stiffness of the heat sink; in other words, graphite heat sinks are more sensitive to breaking when dropped or impacted by other objects. While mechanical and vibration testing, thermal cycling, material characterization, modeling, and geometry optimization will be a subject of the future research, this study is considered a first step in this endeavor.

## Acknowledgment

This work was supported by the NSERC CUI2I grant number 470927-14. The first author would like to thank everyone at the Laboratory for Alternative Energy Conversion for their support and suggestions, and especially Jerry Liu for the help with the measurement automation and data collection.

## References

- [1] X. H. Wei, L. Liu, J. X. Zhang, J. L. Shi, and Q. G. Guo, "Mechanical, electrical, thermal performances and structure characteristics of flexible graphite sheets," *J. Mater. Sci.*, vol. 45, no. 9, pp. 2449–2455, 2010.
- [2] R. Liu, J. Chen, M. Tan, S. Song, Y. Chen, and D. Fu, "Anisotropic high thermal conductivity of flexible graphite sheets used for advanced thermal management materials," *ICMREE 2013 - Proc. 2013 Int. Conf. Mater. Renew. Energy Environ.*, vol. 1, pp. 107–111, 2013.
- [3] M. Inagaki, F. Kang, M. Toyoda, H. Konno, M. Inagaki, F. Kang, M. Toyoda, and H. Konno, "Chapter 16 – Highly Oriented Graphite with High Thermal Conductivity," in *Advanced Materials Science and Engineering of Carbon*, 2014, pp. 363–386.
- [4] M. Smalc, G. Shives, G. Chen, S. Guggari, J. Norley, and R. A. Reynolds, "Thermal Performance of Natural Graphite Heat Spreaders," in *Advances in Electronic Packaging, Parts A, B, and C*, 2005, pp. 79–89.
- [5] Y. Xiong, M. Smalc, J. Norley, J. Chang, H. Mayer, P. Skandakumaran, and B. Reis, "Thermal tests and analysis of thin graphite heat spreader for hot spot reduction in handheld devices," *2008 11th IEEE Intersoc. Conf. Therm. Thermomechanical Phenom. Electron. Syst. I-THERM*, pp. 583–590, 2008.
- [6] A. Shooshtari, J. Kahn, A. Bar-Cohen, S. Dessiatoun, M. Ohadi, M. Getz, and J. Norley, "The Impact of a Thermal Spreader on the Temperature Distribution in a Plasma Display Panel," in *Thermal and Thermomechanical Proceedings 10th Intersociety Conference on Phenomena in Electronics Systems, 2006. IOTHERM 2006.*, pp. 395–401.
- [7] Y. Taira, S. Kohara, and K. Sueoka, "Performance improvement of stacked graphite sheets for cooling applications," *Proc. - Electron. Components Technol. Conf.*, pp. 760–764, 2008.
- [8] S. Ono, H. Nagano, Y. Nishikawa, M. Mishiro, S. Tachikawa, and H. Ogawa, "Thermophysical Properties of High-Thermal-Conductivity Graphite Sheet and Application to Deployable/Stowable Radiator," *J. Thermophys. Heat Transf.*, vol. 29, no. 2, pp. 403–411, 2015.
- [9] T. Icoz and M. Arik, "Light weight high performance thermal management with advanced heat sinks and extended surfaces," *IEEE Trans. Components Packag. Technol.*, vol. 33, no. 1, pp. 161–166, 2010.
- [10] D. Sabatino and K. Yoder, "Pyrolytic graphite heat sinks: A study of circuit board applications," *IEEE Trans. Components, Packag. Manuf. Technol.*, vol. 4, no. 6, pp. 999–1009, 2014.
- [11] G. Chen, J. Capp, G. Getz, D. Flaherty, and J. Norley, "Optimum Design of Heat Sinks Using Non-Isotropic Graphite Composites," in *Heat Transfer: Volume 3*, 2003, pp. 489–494.
- [12] G. Shives, J. Norley, G. Chen, and J. Capp, "Comparative Thermal Performance Evaluation of Graphite/Epoxy Fin Heat Sinks," in *Thermal and Thermomechanical Phenomena in Electronic Systems, 2004. IOTHERM '04*, 2004, pp. 410–417.
- [13] E. E. Marotta, M. J. Ellsworth, J. Norley, and G. Getz, "The Development of a Bonded Fin Graphite/Epoxy Heat Sink for High Performance Servers," in *2003 International Electronic Packaging Technical Conference and Exhibition, Volume 2*, 2003, pp. 139–146.
- [14] "3M™ Thermally Conductive Adhesive Transfer Tapes 8805, 8810, 8815, 8820," 2015. [Online]. Available: <http://multimedia.3m.com/mws/media/1221190/3m-thermally-conductive-adhesive-transfer-tapes-8800-series.pdf>. [Accessed: 14-Dec-2016].